

AD _____

Award Number: W81XWH-04-1-0197

TITLE: Genomic Approaches for Detection and Treatment of Breast Cancer

PRINCIPAL INVESTIGATOR: Stephen J. Elledge, Ph.D.

CONTRACTING ORGANIZATION: Brigham and Women's Hospital
Boston, MA 02115

REPORT DATE: July 2008

TYPE OF REPORT: Annual

PREPARED FOR: U.S. Army Medical Research and Materiel Command
Fort Detrick, Maryland 21702-5012

DISTRIBUTION STATEMENT: Approved for Public Release;
Distribution Unlimited

The views, opinions and/or findings contained in this report are those of the author(s) and should not be construed as an official Department of the Army position, policy or decision unless so designated by other documentation.

REPORT DOCUMENTATION PAGE				Form Approved OMB No. 0704-0188	
Public reporting burden for this collection of information is estimated to average 1 hour per response, including the time for reviewing instructions, searching existing data sources, gathering and maintaining the data needed, and completing and reviewing this collection of information. Send comments regarding this burden estimate or any other aspect of this collection of information, including suggestions for reducing this burden to Department of Defense, Washington Headquarters Services, Directorate for Information Operations and Reports (0704-0188), 1215 Jefferson Davis Highway, Suite 1204, Arlington, VA 22202-4302. Respondents should be aware that notwithstanding any other provision of law, no person shall be subject to any penalty for failing to comply with a collection of information if it does not display a currently valid OMB control number. PLEASE DO NOT RETURN YOUR FORM TO THE ABOVE ADDRESS.					
1. REPORT DATE 1 July 2008		2. REPORT TYPE Annual		3. DATES COVERED 1 July 2007 – 30 June 2008	
4. TITLE AND SUBTITLE Genomic Approaches for Detection and Treatment of Breast Cancer				5a. CONTRACT NUMBER	
				5b. GRANT NUMBER W81XWH-04-1-0197	
				5c. PROGRAM ELEMENT NUMBER	
6. AUTHOR(S) Stephen J. Elledge, Ph.D. E-Mail: chanes@rics.bwh.harvard.edu				5d. PROJECT NUMBER	
				5e. TASK NUMBER	
				5f. WORK UNIT NUMBER	
7. PERFORMING ORGANIZATION NAME(S) AND ADDRESS(ES) Brigham and Women's Hospital Boston, MA 02115				8. PERFORMING ORGANIZATION REPORT NUMBER	
9. SPONSORING / MONITORING AGENCY NAME(S) AND ADDRESS(ES) U.S. Army Medical Research and Materiel Command Fort Detrick, Maryland 21702-5012				10. SPONSOR/MONITOR'S ACRONYM(S)	
				11. SPONSOR/MONITOR'S REPORT NUMBER(S)	
12. DISTRIBUTION / AVAILABILITY STATEMENT Approved for Public Release; Distribution Unlimited					
13. SUPPLEMENTARY NOTES					
14. ABSTRACT Not provided					
15. SUBJECT TERMS Breast Cancer					
16. SECURITY CLASSIFICATION OF:			17. LIMITATION OF ABSTRACT	18. NUMBER OF PAGES	19a. NAME OF RESPONSIBLE PERSON
a. REPORT	b. ABSTRACT	c. THIS PAGE			USAMRMC
U	U	U	UU	25	19b. TELEPHONE NUMBER (include area code)

Table of Contents

Introduction	4
Body	4
Key Research Accomplishments	19
Reportable Outcomes	22
Conclusions	23
References	24

Introduction

A key part of our research plan has been the development and use of retroviral vectors expressing RNA interference RNAs to identify human genes involved in causing or restraining cancer. In our first progress reports we described our efforts to develop shRNA libraries and showed they could be used to identify tumor suppressors. Ultimately our goal is to screen of complex pools of shRNA expressing retroviruses each marked with a bar code that allows the results of the screen to be read out by microarray hybridization. We demonstrated this could be accomplished in enrichment screens for shRNAs that caused cellular transformation and growth in soft agar. However, a key goal has been to identify shRNAs that debilitate or kill cancer cells. In order for this to be possible in complex pools, it is imperative that each vector knock down its target with high penetrance. We have successfully achieved this level of knockdown and can now see particular shRNA expressing viruses drop out of complex pools. We have used this methodology to search for genes whose knockdown enhance the proliferative capacity of normal breast epithelial cells, i.e. candidate tumor suppressors and genes whose knockdown are cancer specific lethals.

Body

Identification of cancer-relevant genes.

Control of REST Degradation

The transcription factor REST/NSRF (RE1-Silencing Transcription Factor) is a master repressor of neuronal gene expression and neuronal programs in non-neuronal lineages¹⁻³. In the course of this grant, we identified REST as a human tumor suppressor in breast epithelial tissues⁴, suggesting that REST regulation may have important physiologic and pathologic consequences. However, the pathways controlling REST have yet to be elucidated. We went forward to further study this problem and found that REST is actually regulated by ubiquitin-mediated proteolysis> We found through an RNAi screen that SCF ^{β TRCP} is an E3 ubiquitin ligase responsible for REST degradation. β TRCP binds and ubiquitinates REST and controls its stability through a conserved phosphodegron. During neural differentiation and in breast cells REST is degraded in a β TRCP-dependent manner. β TRCP is required for proper neural differentiation only in the presence of REST, indicating that β TRCP facilitates this process through degradation of REST. Conversely, failure to degrade REST attenuates differentiation. Furthermore, we find that β TRCP overexpression, which is common in human epithelial cancers including breast, causes oncogenic transformation of human mammary epithelial cells and this pathogenic function requires REST degradation. Thus, REST is a key target in β TRCP-driven transformation and the β TRCP-REST axis is a new regulatory pathway controlling neurogenesis.

REST levels decline during differentiation of embryonic stem cells to neural stem and progenitor cells⁵ and REST is unstable in breast epithelial cells, consistent with a role for REST in restraining neuronal gene expression programs and that its levels are critically regulated in breast tissue. This decrease in neurogenesis results from a 3-fold reduction in REST half-life (Fig. 1a), suggesting that a regulatory pathway controls REST degradation during early neural differentiation. To determine whether ubiquitination is involved, REST was evaluated for ubiquitin-modification *in vivo*. Immunoprecipitation of HA-ubiquitin revealed slower migrating

species of REST suggestive of polyubiquitination (Fig. 1b, lane 3). REST also precipitated with an HA-ubiquitin mutant lacking all lysines except K48 (Fig. 1b, lane 4), suggesting REST is K48 polyubiquitinated which promotes degradation.

To search for the E3 ubiquitin ligase for REST, we began with the SCF superfamily of ligases⁶. Each SCF family contains a common Cullin scaffold that is required for ligase function. Notably, coexpression of a dominant negative Cullin-1 (Cul1) mutant resulted in a dramatic increase (11-fold) in REST levels, indicating that one or more Cul1-containing ligases negatively regulate REST abundance.

F-box proteins act as substrate receptors for the SCF^{7,8}. To determine which F-box proteins are required for REST turnover, we established a system for monitoring REST abundance in a high-throughput manner using an mRFP-REST fusion protein. Similar to endogenous REST, mRFP-REST was unstable, and its abundance increased upon inhibition of Cul-1. To identify the F-box proteins regulating REST, individual siRNAs targeting each F-box protein (4 siRNAs/gene) were cotransfected with a plasmid encoding mRFP-REST, and changes in cellular fluorescence were monitored by flow cytometry. siRNAs that increased fluorescence >2 standard deviations from the mean were retested in triplicate for their effects on both mRFP and mRFP-REST to identify siRNAs that specifically alter REST stability (Fig. 1c). This approach identified FBW4 and β TRCP2. Notably, multiple siRNAs targeting additional sequences within FBW4 and β TRCP2 also increased mRFP-REST abundance (Fig. 1d), confirming the specificity of the siRNAs. Supporting this conclusion, coexpression of a dominant negative β TRCP mutant (lacking the F-box) also increased REST levels (data not shown).

β TRCP2 and FBW4 may control REST abundance by direct ubiquitination of REST or by modulating upstream regulators of REST. β TRCP2, but not FBW4, was capable of binding REST in cells (Fig. 1e), suggesting that FBW4-mediated regulation is indirect. The highly homologous β TRCP1 also interacted with REST (Fig. 1e and data not shown), consistent with previous reports that β TRCP1 and β TRCP2 have similar substrate specificities and frequently function redundantly^{9,10}. Importantly, endogenous β TRCP and REST interact in cells (data not shown), and REST was polyubiquitinated by SCF β TRCP1 *in vitro* (Fig. 1f), suggesting that SCF β TRCP regulates REST by direct ubiquitination. In agreement, stable expression of β TRCP-shRNA (targeting β TRCP1 and β TRCP2) in both human mammary epithelial cells (HMECs) and NIH3T3 cells resulted in a moderate but reproducible increase in REST protein abundance and half-life (Fig. 1g, lanes 2 and 3), indicating that endogenous REST is regulated by β TRCP. These data indicate that SCF β TRCP controls REST by ubiquitin-mediated destabilization.

Fig. 1

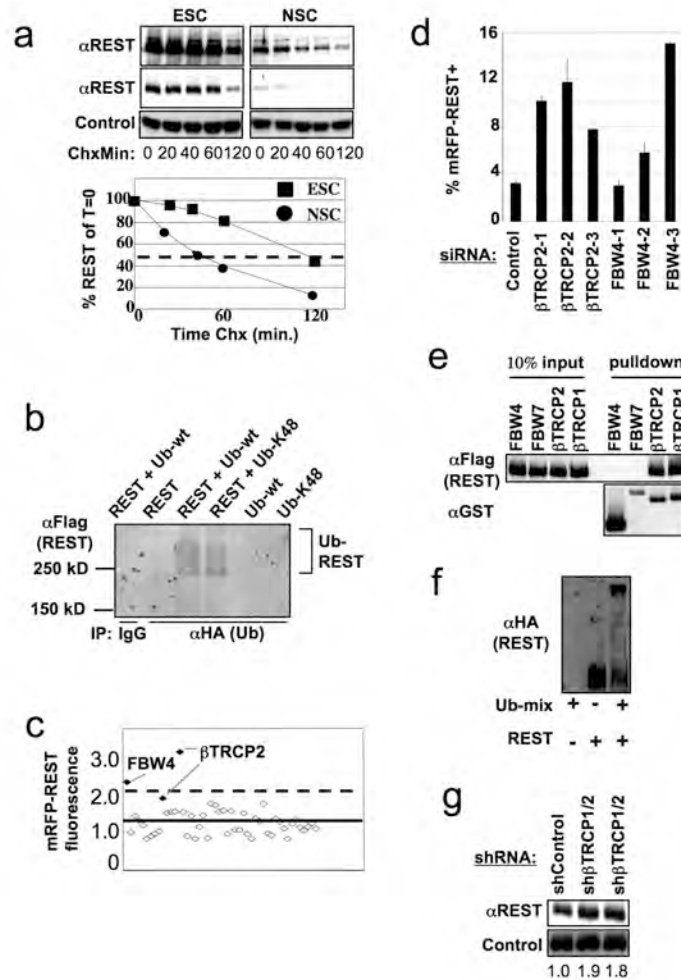


Figure 1

Identification of bTRCP and FBW4 ubiquitin ligases as regulators of REST stability. a, Embryonic stem cells (ESC) or Neural Stem Cells (NSC) were examined for REST protein half-life in a cycloheximide (Chx) timecourse. Quantitation of relative REST levels in lower panel (dotted line denotes half-life). b, 293T cells were transfected with plasmids expressing Flag-REST, HA-ubiquitin, and/or HA-ubiquitin-K48 as indicated, immunoprecipitated with HA-specific antibodies or control IgG, and analyzed by aFlag immunoblot. c, siRNA screen for regulators of mRFP-REST. d, siRNAs targeting bTRCP2 or FBW4 sequences independent from library-derived siRNAs were tested for effects on mRFP-REST fluorescence (n=3, error bars +/- s.d.). e, Coimmunoprecipitation of GST-F-box fusion proteins and Flag-REST from mammalian cells. f, *in vitro* ubiquitination of HA-REST by SCF^{bTRCP}. g, Human mammary epithelial cells expressing control shRNA or shRNA-targeting human bTRCP1 and bTRCP2 were analyzed by aREST immunoblot. Two-independent infections with bTRCP-shRNA are shown. Quantitation of relative REST levels is shown below each lane.

SCF^{βTRCP} binds substrates in a phosphorylation-dependent manner^{6,10-14}. Consistent with this, λ-phosphatase treatment abolished the interaction between REST and βTRCP and this was prevented by λ-phosphatase inhibitors (Fig. 2a). Notably, a dominant negative frame-shift mutant of REST found in human colon cancer cells⁴ failed to interact with βTRCP and exhibited substantially increased stability in cells, indicating the C-terminal half of REST is required for βTRCP recognition. Analysis of this region revealed a sequence highly similar to the phosphodegron found in Cdc25A, a well documented βTRCP-substrate^{11,12} (Fig. 2b). This putative degron includes a conserved DpSG motif that constitutes a critical interaction element within phosphodegrons for βTRCP¹⁵. Mass spectrometry was used to examine phosphorylation of REST within this region. To enable tryptic digestion of the peptide of interest, a N1022R substitution was introduced into REST that does not alter interaction with βTRCP or protein stability in cells (data not shown). His-tagged REST^{N1022R} was co-expressed with dominant-negative Cull1 in 293T cells and purified under denaturing conditions (data not shown). Analysis of phosphopeptides in REST^{N1022R} demonstrated that S1027 and S1030 within the MSEGSDDDSGLHGARPVPQESSR peptide are phosphorylated both singly and in combination.

To test the ability of the candidate REST-degron to interact with βTRCP, peptides spanning the degron were synthesized with phosphates at serines 1024, 1027, and 1030 alone or in combination. Individual serine-phosphorylation facilitated weak (S1030) or no interaction (S1024 or S1027) with βTRCP (Fig. 2d) while peptides phosphorylated in combination at S1027+S1030 or S1024+S1027+S1030 associated with βTRCP (but not Fbw4) with an efficiency comparable to the well-established IκB phosphodegron peptide (Fig. 2d and data not shown). Mutation of each serine to alanine in the context of full-length REST resulted in decreased binding to βTRCP, and combined mutation of these critical serines completely abrogated the interaction with βTRCP (Fig. 2c). Notably, degron-mutant REST was substantially more stable than wild-type REST in cells (Fig. 2e). These data support the hypothesis that phosphorylation of the REST degron primes ubiquitination by SCF^{βTRCP}, thereby promoting REST degradation.

Fig. 2

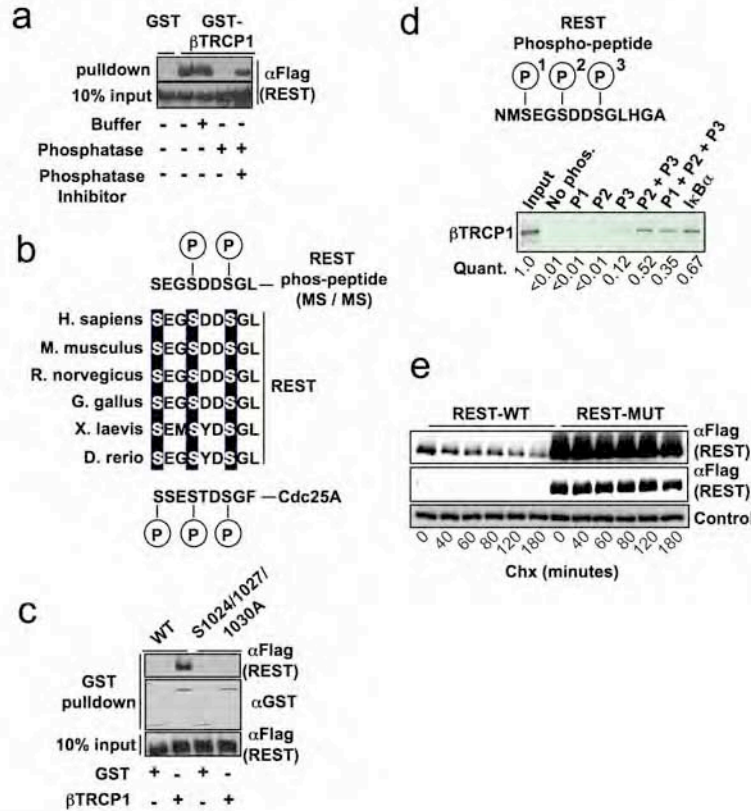


Figure 2

A conserved phosphodegion in REST is required for regulation by β TRCP. **a**, 293T cells were transfected with GST, GST- β TRCP1 or Flag-REST expression plasmids. Flag-REST lysates were treated with buffer, λ -phosphatase, or λ -phosphatase + phosphatase-inhibitor as indicated. Flag-REST lysates were then mixed with GST- or GST- β TRCP1 lysates, precipitated with glutathione beads and immunoblotted with α Flag antibodies. **b**, Phosphorylation of the conserved REST degion *in vivo*. Sequence alignments of REST proteins (*Hs* REST residues 1024-1032) from several species and the phosphodegion from *Hs* CDC25A. Phospho-serines within the REST degion identified by MS/MS are shown in upper sequence. **c**, 293T cells expressing the indicated combinations of GST, GST- β TRCP1 (denoted on bottom), and Flag-REST mutants (denoted at top). GST-bound complexes were immunoblotted with α Flag (upper and lower panels) or α GST (middle). **d**, 35 S- β TRCP1 was transcribed/translated *in vitro* and incubated with biotin-conjugated peptides spanning the REST degion (unphosphorylated or phosphorylated) or the I κ B degion (phosphorylated). Peptide-associated-proteins were precipitated with streptavidin-conjugated beads, analyzed by SDS-PAGE, and quantified using a phosphoimager. Peptide sequence spanning the REST degion is shown in the top panel. **e**, 293T cells expressing wild-type or degion-mutant Flag-REST cDNAs were examined for Flag-REST protein half-life in a cycloheximide (Chx) timecourse.

The role of β TRCP in degradation of the REST tumor suppressor predicts that β TRCP overproduction might transform human cells. To examine this prediction, HMECs stably expressing human telomerase catalytic subunit (hTERT) and the SV40 LT oncogene ("TLM-HMECs,"¹⁶) were transduced with a control or GFP- β TRCP1-expressing retrovirus. Stable ectopic expression of β TRCP1 resulted in reduced REST abundance (Fig. 3a) and robust anchorage-independent proliferation (Fig. 3b), thus phenocopying REST loss-of-function⁴. This is consistent with a transgenic mouse model in which ectopic β TRCP1 expression in the mammary gland produced advanced breast cancer¹⁷. To determine whether REST degradation is critical for β TRCP1-mediated transformation, TLM-HMECs stably expressing β TRCP1 were transduced with retroviruses expressing wild-type or degron-mutant REST. Exogenous REST expression did not alter proliferation on an adhesive cell culture surface (Fig. 3c). In contrast, β TRCP1-induced anchorage-independent proliferation was severely impaired by restoring REST expression (Fig. 3d). Consistent with its increased stability, degron-defective REST suppressed β TRCP1-transformation more efficiently (Fig. 3d data not shown). These data implicate REST as an essential target in β TRCP-driven oncogenic transformation.

While REST is a well documented regulator of neuronal gene expression and has been proposed to restrain several steps in neurogenesis (reviewed in ³), its role in neurogenesis has not been tested genetically. Thus, we used embryonic stem (ES) cells to genetically examine the roles of REST and β TRCP in the differentiation program of neural stem and progenitor cells (reviewed in ¹⁸). For this we employed ES cells in which eGFP was recombined into the Sox1 locus^{19,20} ("46c cells"), a well characterized marker of early neural differentiation *in vitro* and *in vivo*.

We first confirmed that endogenous REST stability is regulated during neural differentiation of 46c cells. As shown in Figure 4a, REST half-life declined 2-fold in differentiated cells, consistent with the decreased REST stability observed in homogeneous neural stem cells (Fig. 1a). This decrease may be driven, in part, by a concomitant 13-fold increase in β TRCP1 expression (Fig. 4b). To test the role of REST and β TRCP in this differentiation program, 46c cells were transfected with control, REST, or β TRCP1 targeting siRNAs alone or in combination, and subsequently cultured in differentiation media and analyzed for neural differentiation by flow cytometric analysis of Sox1:eGFP fluorescence. Inactivation of REST promoted differentiation, correlating with the efficiency of REST knockdown (Fig. 3c, thus providing the first genetic evidence that REST negatively regulates early neural differentiation. Conversely, siRNAs that suppress β TRCP1 expression >90% attenuate differentiation into the neural lineage (Fig. 3c). These results were confirmed in multiple time points (data not shown) and with multiple siRNAs. Importantly, simultaneous REST+ β TRCP1 knockdown increased Sox1:eGFP-positive cells >5-fold relative to β TRCP1-siRNA alone (Fig. 4c), showing REST reduction restores neural differentiation in the absence of β TRCP. Similar results were observed by measuring the abundance of an independent neuronal marker, TUBB3 (Fig. 4d). Thus, down regulation of REST is a critical function of β TRCP during early neural differentiation.

Fig. 3

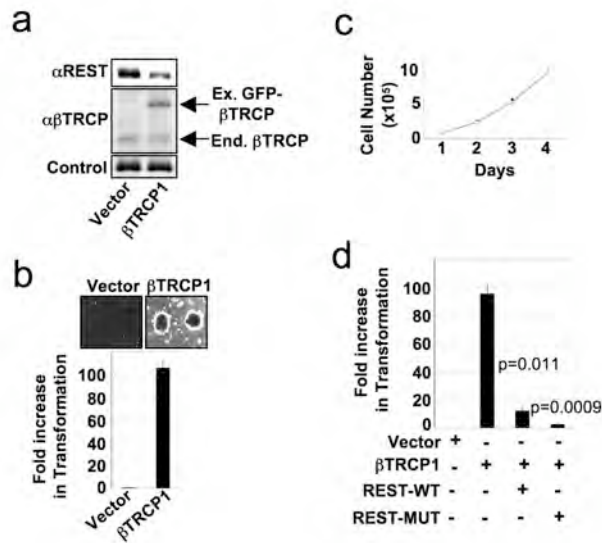


Figure 3

TRCP targets REST during oncogenic transformation. **a**, TLM-HMECs were transduced with control or GFP-bTRCP1-expressing retroviruses. Lysates were probed with antibodies against REST (upper panel), bTRCP (middle panel), or Vinculin (lower panel). **b**, Cells from **a** were analyzed for anchorage-independent colony formation. Assays were performed in quadruplicate (error bars +/- s.d.). Representative of 3 independent experiments is shown. **c**, HMECs were transduced with retroviruses expressing wild-type REST (REST-WT), degron-mutant REST (REST-MUT), and/or bTRCP1. Cell numbers were monitored for 4 days after plating on tissue-culture dishes. (open circles: vector-1+vector-2, closed circles: bTRCP1, open triangles: bTRCP1+vector-2, closed diamonds: bTRCP1+REST-WT, open squares: bTRCP1+REST-MUT) **d**, Cells from **c** were assessed for anchorage-independent colony formation. Assays were performed in triplicate (error bars +/- s.d.). Representative of 2 independent experiments is shown.

These data support the model that βTRCP regulates neural differentiation by facilitating REST degradation and predicts that a non-degradable REST would impede neural differentiation. To test this, we first examined the stability of wild-type or degron-mutant REST expressed in the context of neural differentiation. In this experiment, REST transgenes were expressed at levels much lower than endogenous REST to prevent alterations in differentiation kinetics (see below). Notably, the stability of endogenous REST and wild-type exogenous REST decreased similarly during neural differentiation (data not shown). In contrast, degron-mutant REST was stable regardless of the cellular differentiation status. To test whether REST stabilization alters neural differentiation, 46c cells were transduced with high-titer retroviruses expressing wild-type or degron-mutant REST, resulting in a 1.5- and 2.6-fold increase in total REST (Fig. 4e). Notably, both transgenes attenuated neural differentiation, with the degron-mutant REST eliciting a more dramatic phenotype (Fig. 4f).

To further demonstrate REST's role in neural differentiation, we employed an independent neural differentiation assay. ES cells stably expressing wild-type or degron-mutant REST were differentiated by formation of embryoid bodies followed by stimulation with retinoic acid, a protocol routinely used to differentiate ES cells into the neuronal lineage²¹. In this context, non-degradable REST suppressed differentiation >5-fold as measured by mRNA expression of Sox1 (Fig. 4g).

The data we generated demonstrate that REST is a labile protein targeted for ubiquitin-dependent proteasomal degradation by SCF^{βTRCP} through a phospho-degron on REST. We showed that SCF^{βTRCP} is a critical regulator of both physiologic and pathologic REST activities, constituting a new pathway controlling neural differentiation and cellular transformation. We provided the first genetic evidence that REST and SCF^{βTRCP} regulate an early stage in neural specification as an inhibitor of neural differentiation. This is likely to be important in epithelial cancers as forced SCF^{βTRCP} activation is known to cause breast cancer when expressed in mouse mammary glands. Our data are consistent with a model in which developmental cues induce degradation of REST, resulting in the derepression of REST targets. The ability of stable REST to inhibit terminal differentiation of neurons also predicts that REST may promote proliferative properties in the neuronal lineage when overproduced or inappropriately stabilized. Consistent with this notion, REST is overexpressed in human medulloblastoma and ectopic REST expression in *v-myc*-immortalized neural stem cells promotes medulloblastoma formation in mice^{22,23}. Thus, the contrasting roles of REST as an oncogene and tumor suppressor are highly dependent on the developmental lineages.

βTRCP is overexpressed and oncogenic in epithelial cancers^{17,24,25} and we identified REST as a key target in this context. This suggests that pharmacologic inhibition of βTRCP may provide a means to restore REST tumor suppressor function in human cancer. The presence of a phosphodegron motif within REST suggests a role for upstream kinase(s) and/or phosphatase(s) that control REST degradation. We propose a model in which differentiation into the neural state is induced by this yet to be discovered signal transduction cascade that targets REST for degradation by SCF^{βTRCP}, acting cooperatively with induction of βTRCP expression during neural differentiation.

Fig. 4

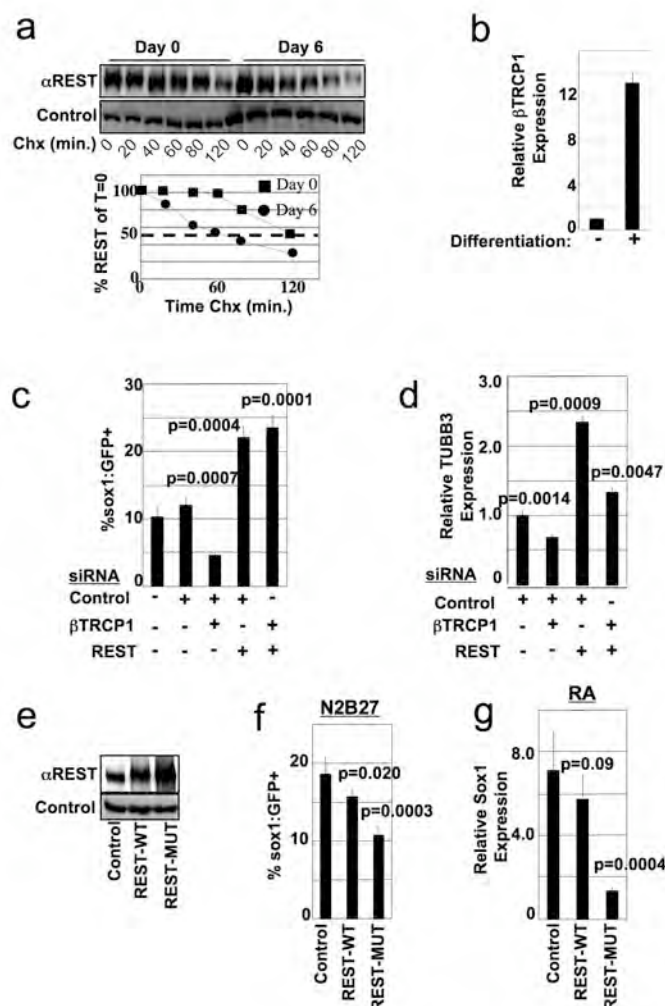


Figure 4

The β TRCP-REST pathway controls neural differentiation. **a**, ES cells differentiated for 0 or 6 days were examined for REST protein half-life in a cycloheximide (Chx) timecourse. Differentiated lysates were analyzed at 3x the concentration of undifferentiated lysates. Quantitation of REST levels is shown in the lower panel. **b**, ES cells were differentiated for 0 or 6 days. β TRCP1 mRNA was analyzed by qRT-PCR, and normalized to GAPDH mRNA abundance. Experiment was performed in triplicate (error bars +/- s.d.). **c**, 46C cells transfected with the indicated combination of siRNAs were differentiated in N2B27 medium and analyzed for Sox1:GFP expression by flow cytometry. Experiments were performed in quadruplicate (error bars +/- s.d.) and is representative of 4 independent experiments. **d**, 46C cells from **c** were analyzed for expression of TUBB3 mRNA by qRT-PCR, and normalized to GAPDH mRNA abundance. Experiments were performed in triplicate (error bars +/- s.d.). **e**, 46C cells expressing control, Flag-REST-WT, or Flag-REST-MUT (triple point mutation in the REST-degion) cDNA were immunoblotted with α REST (upper panel) or α vinculin (lower panel) antibodies. Note: In this experiment, exogenous REST was expressed at levels higher than endogenous REST. **f**, 46C cells from **e** were cultured in N2B27 differentiation medium and analyzed for Sox1:GFP fluorescence. This experiment was performed in sextuplicate (error bars +/- s.d.) and is representative of 2 independent experiments. **g**, ES cells were infected as in **e**, differentiated into the neural lineage using an embryoid body-retinoic acid protocol, and analyzed for Sox1 mRNA by qRT-PCR (normalized to GAPDH mRNA abundance). Experiment was performed in triplicate (error bars +/- s.d.).

Conversely, hyperactivation of such pathway(s) priming REST degradation may be oncogenic in epithelial tissues and thus serve as new therapeutic targets in cancers with compromised REST function. Thus, exploration of these pathways will likely provide new opportunities for modulating neural stem cell and cancer cell behavior. We need to find the kinase that regulates REST as it will be a potential oncogene.

We also participated in a collaboration with Yang Shi's lab who was working on methyltransferases. They found a protein CDYL that also binds REST and Methyltransferases to negatively regulate target gene expression through REST binding to promoters. We showed with them that CDYL is also a tumor suppressor candidate and knocking down CDYL expression transforms HMECs.

Identification of novel tumor suppressor genes

As we have described previously, we have developed viral shRNA libraries targeting the entire human genome to explore loss-of-function phenotypes in mammalian systems and have applied these libraries towards identification of novel tumor suppressor genes. With recent improvements in our library, we have revisited our search for novel tumor suppressor genes in breast cancer by using a genome-wide enrichment screen to identify genes whose knockdown increases proliferation and/or survival of normal human mammary epithelial cells (HMECs).

A detailed description of our HMEC enrichment screen is illustrated in Figure 8. Early passage HMECs used for the screen were obtained from a reduction mammaplasty and immortalized by expression of hTERT and spontaneous silencing of p16. To screen the entire genome-wide library of ~80,000 shRNAs, screens were performed in 6 separate pools of ~13,000 shRNAs. HMECs were infected in triplicate with a representation of 1000 cells per shRNA at an MOI of 2 viruses per cell. Initial reference samples were collected 72 hours post-infection. The remaining cells were puromycin-selected for 4 days and propagated with a representation of ≥ 1000 cells per shRNA maintained at each passage. Cells were collected as the end samples after ~7 population doublings (PDs). Probes were prepared from both samples, and Cy3- or Cy5-labeled probes were competitively hybridized to half-hairpin barcode microarrays to measure the change in representation of each shRNA over time.

Statistical analysis indicate that most probes consistently yielded signals >2-fold above the mean background of negative control probes across all triplicates. The correlations among the initial samples across triplicates and between the initial and end samples within each replica were high, indicating high reproducibility and maintenance of representation. As expected, most shRNAs showed little change over the time course of the screen. However, using statistical analysis for microarray (SAM) with a false discovery rate (FDR) of 5%, we observed that the abundance of 4257 shRNAs against 3653 genes were increased > 2-fold over the course of the screen, indicating these shRNAs increase proliferation and/or survival of HMECs.

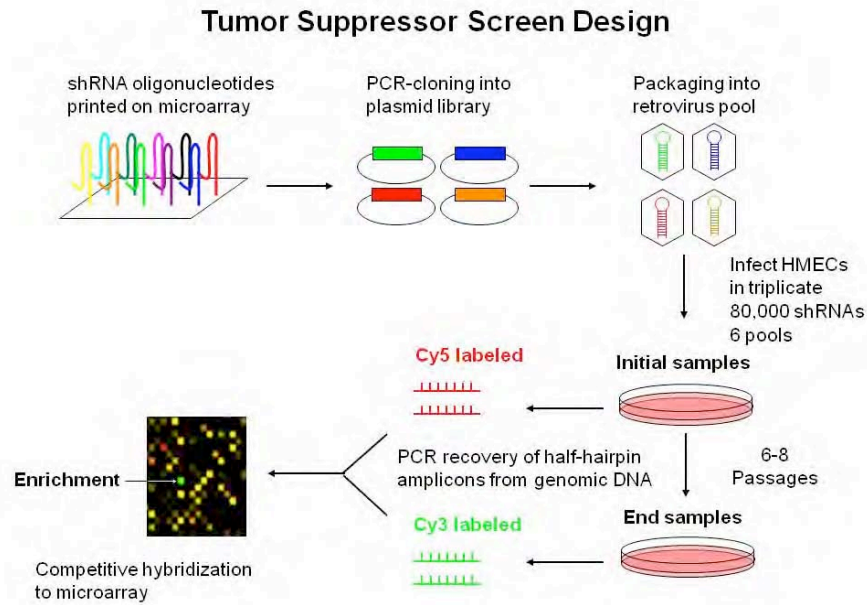


Figure 8.

Tumor suppressor screen design. A genome-wide enrichment screen was performed in human mammary epithelial cells for shRNAs against genes whose knockdown increases proliferation or cell survival. Such genes are novel tumor suppressor candidates.

Many of the genes whose knockdown lead to increased proliferation and/or survival are known tumor suppressor genes or key mediators of proliferation and apoptotic pathways. For example, shRNAs against genes encoding the tumor suppressors Rb, PTEN, and p53 were all increased over the course of the screen. Furthermore, shRNAs against proliferation genes, such as those encoding the Rb-like proteins p107 and p130 and cyclin dependent kinase inhibitors p21, p27, and p57, as well as shRNAs against pro-apoptotic genes, such as those encoding caspase 3, caspase 6, and Apaf-1 scored as well.

We are currently using a multi-color competition assay (MCA) to validate shRNAs which have scored in our screen and determine whether knockdown of candidate genes increases proliferation and/or survival. Thus far, we have examined 142 candidate shRNAs against 123 known genes that scored in our screen for their effect on cell proliferation and/or survival. Using the MCA assay, 58 of 142 candidate shRNAs (40%) validated to increase proliferation and/or survival compared to FF2 control shRNAs over the 6 day assay. We are currently investigating these genes to determine the mechanisms by which their knockdown increases proliferation and/or survival and whether they are novel tumor suppressors. Furthermore, we are using genomic profiling of tumor samples to determine whether these genes are located in focal deletion regions, which would suggest that they are involved in tumor suppression.

Identification of breast cancer-specific lethal genes

Genetic loss-of-function screening to identify genes that are essential to cancer cell proliferation and survival is a powerful and complementary approach to large sequencing efforts and is expected to provide many potential cancer drug targets. Towards this end, we have performed lethality screens to identify genes that are selectively required for proliferation and survival of breast cancer cells but not normal mammary epithelial cells, which we call Breast Cancer Lethal (BCAL) genes. For lethality screens, the abundance of shRNAs targeting genes that are essential for cell viability will be reduced following cell passaging and will thus “drop-out” of the shRNA population. By comparing each shRNA’s abundance in an initial cell population taken shortly after retroviral shRNA library infection to its abundance in samples taken after several cell population doublings, lethal shRNAs can be identified. Additionally, comparisons between the shRNA lethality profiles of breast cancer cells and normal human mammary epithelial cells can identify BCAL genes (Figure 9).

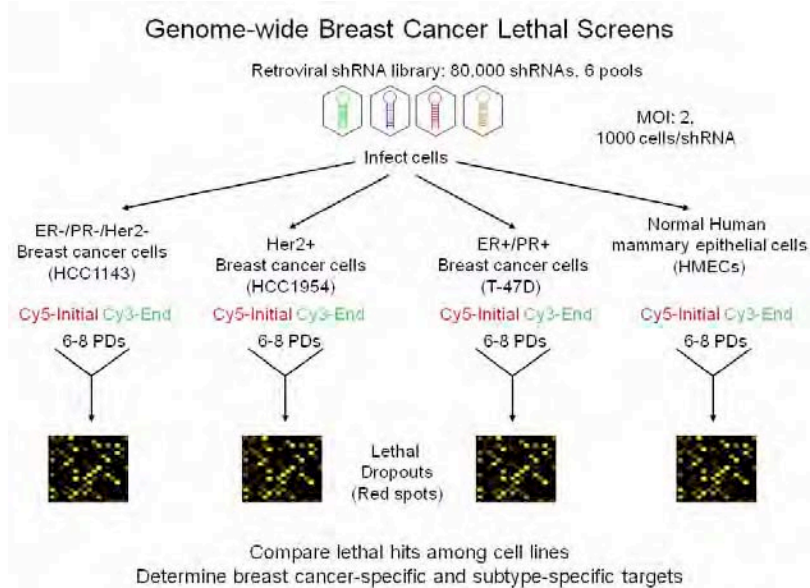


Figure 9.
Breast cancer lethal screen design.
A genome-wide lethality screen was performed in three breast cancer cell lines and one normal human mammary epithelial cell line for shRNAs against genes whose knockdown decreases viability of breast cancer but not normal cells. Such genes are novel cancer drug targets.

To identify BCAL genes, we have performed highly-parallel, genome-wide, pooled, shRNA lethality screens in three breast cancer (HCC1954, HCC1143, T47D) and one normal mammary epithelial (HMEC) cell lines. Cells were infected in triplicate with the entire genome-wide library of ~80,000 shRNAs in 6 separate pools of ~13,000 shRNAs/pool. Cells were infected in triplicate with a representation of 1000 cells per shRNA at an MOI of 2 viruses per cell. Initial reference samples were collected 72 hours post-infection. The remaining cells were puromycin-selected for 4 days and propagated with a representation of ≥ 1000 cells per shRNA maintained at each passage. Cells were collected as the end samples after ~7 population doublings (PDs). Probes were prepared from both initial and end samples, and Cy3- or Cy5-labeled probes were competitively hybridized to half-hairpin barcode microarrays to measure the change in representation of each shRNA over time.

Statistical analysis indicate that most probes consistently yielded signals >2-fold above the mean background of negative control probes across all triplicates. The correlations among the initial samples across triplicates and between the initial and end samples within each replica were high, indicating high reproducibility and maintenance of representation. To identify cancer-specific lethal shRNAs, we utilized statistical analysis for microarray (SAM) with a false discovery rate (FDR) of 10% as well as several fold change cutoffs. For a given shRNA to score as a BCAL shRNA, its abundance decreased > 2-fold in one of the three breast cancer cell lines, but was not decreased > 2-fold in HMECs. Furthermore, a BCAL shRNA displayed > 1.8 fold difference in abundance between the normal and breast cancer cell line. We identified 3787 shRNAs against 3410 genes that met these BCAL criteria. These shRNAs and genes were further classified into 4 groups: “pan” BCAL shRNAs that were selectively lethal to 2 or more breast cancer cell lines, and HCC1954, HCC1143, and T47D cell type-specific BCAL shRNAs that were selectively lethal to a single breast cancer cell line. We are currently validating whether knockdown of candidate BCAL genes leads to reduced viability of breast cancer cell lines but not normal HMECs using a Cell Titer Glo viability assay. Furthermore, we are investigating these candidates using mechanistic studies to determine how their reduction leads to cancer cell lethality. We expect these BCAL genes will reveal novel oncogene or non-oncogene additions of breast cancer cells that can lead to new therapeutic targets for breast cancer.

Anti-tumor Antibody profiling

Anti-tumor auto-antibodies have been proposed to be highly sensitive and specific biomarkers for early cancer detection. To identify antibody binding profiles specific for cancer patients, a number of groups have utilized phage display, a high- throughput affinity assay. In this approach, libraries of peptides or protein fragments are displayed on the surface of a bacteriophage, thereby allowing a proteomic screen for binding properties of a patient’s antibody repertoire. Previous efforts towards auto-antibody biomarker discovery using phage display have used either random peptides or tumor-derived cDNA libraries to “pan” displayed peptides against patient sera. Such studies have been difficult to interpret, however, since resulting “hits” are frequently out of frame or derived from noncoding sequences.

Our novel strategy has been to encode the human “peptidome” as a set of individual DNA microarray-derived oligonucleotides. We have generated a library of approximately 467,000 oligos that tile the entire set of human open reading frames. For phage display, the oligos were cloned into the T7Select (Novagen) system, allowing for low copy number display fused to the T7 coat protein, 10B. The library was then extensively characterized by sequencing several hundred individual phage clones at random. As we reported last year, 74% of our phage population encodes in-frame peptides, and 55% of the population expresses completely correct sequences. This phage library is unique in several respects. First, this is the first example of a synthetic phage display library encoding protein fragments from microarray-derived oligonucleotides. Second, this library is the only example of a normalized representation of the human peptidome. The alternative random peptide and cDNA derived libraries are much less powerful from a cancer biomarker screening standpoint.

Autoantibody Profiling Strategy

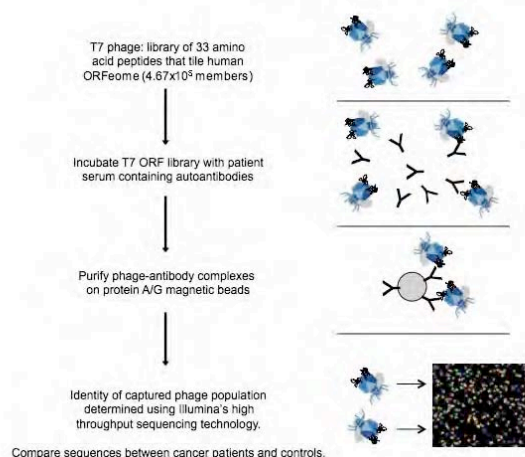


Figure 10.

Novel approach to patient autoantibody profiling. T7-Peptidome library is mixed with patient antibodies and specific complexes are allowed to form. Complexes are purified on magnetic protein A/G beads. High throughput sequencing is utilized to identify captured phage, and profiles are compared between patients.

The sensitivity of our screen for auto-antibodies associated with breast cancer can be determined by the degree of specific enrichment that we are able to obtain by immunoprecipitating antibody-bound phage. To this end, we have optimized the conditions for enrichment since our last report. By diluting a FLAG-tagged T7 phage (1:1000) into a native phage population and diluting an anti-FLAG antibody (1:1000) into a non-specific isotype control antibody, we were able to mimic the high complexity of our assay with just four variables. We optimized for enrichment (measured quantitatively with the plaque lift assay) by systematically varying the following parameters: T7 phage concentration, antibody concentration, time of immunoprecipitation, and number of washes before phage elution. The concentrations of phage and antibody during complex formation were assumed to be dependent on each other, and were thus optimized simultaneously (Figure 11). We successfully optimized all 4 parameters, allowing for a FLAG phage enrichment factor of over 4000-fold showing the basic premise of the screen is sound and we should be able to screen breast serum samples.

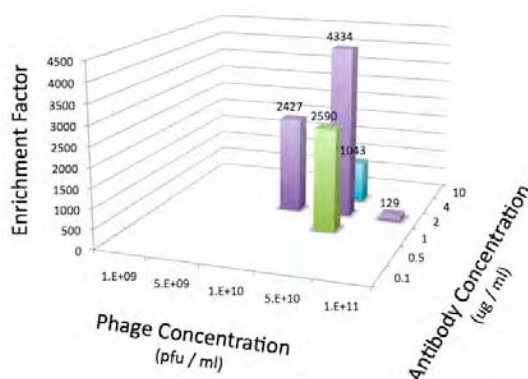


Figure 11.

Simultaneous optimization of phage concentration and antibody concentration for maximum enrichment of specific phage immunoprecipitation.

After optimizing enrichment conditions, we performed our optimized immunoprecipitation assay on our synthetic phage library to validate our enrichment protocol. To this end, we immunoprecipitated a pool of our library with a combination of 9 antibodies, all of which are directed against the C-termini of different human proteins. This pool consisted of 27,000 unique

phage displaying the C-terminal peptidome. Finally, a plaque lift of the immunoprecipitated phage were immunoblotted with the same mix of C-terminal antibodies (Figure 12). Whereas there were apparently no “hits” on a plaque lift derived from the input library, we observed a large fraction of positively staining plaques on the immunoprecipitated sample. Of the thirty hits that were sequenced, all of these corresponded to peptides specifically targeted by the C-terminally-directed input antibodies, suggesting that our optimized enrichment protocol is highly selective for specific interactions.

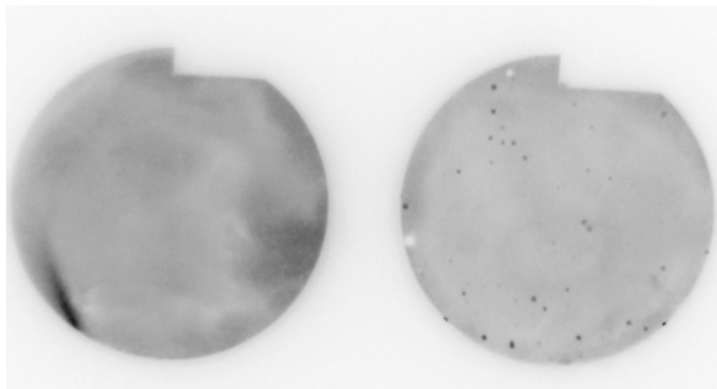


Figure 12.
Plaque lifts of the C-terminal peptidome libraries, stained with a pool of 9 anti-C-terminal protein antibodies. Blot on the left is from the input library, and blot on the right is from the phage immunoprecipitated with the same pool of antibodies.

As reported last year, we had experienced difficulty using microarrays to uniquely identify the phage species present in a given sample. This was largely due to the fact that our probe design was highly constrained by the sequences of the oligonucleotide inserts. A high degree of cross-hybridization was observed, which compromised the quality of our data. The alternative, high throughput sequencing of the oligo inserts, is expensive and therefore prohibitive for a screen of >100 samples. We have therefore developed an indexing scheme to allow multiplexing of samples during high throughput sequencing, thereby reducing the cost per sample (Figure 13). Thus far, we have begun our biomarker screen by immunoprecipitating the C-terminal peptidome phage pool using sera from a breast cancer patient and a healthy volunteer. The results of this simplified experiment will allow us to calculate the signal to noise inherent to our system, and thus estimate the level of allowable multiplexing which will not significantly compromise the quality of the data. Once this pilot phage IP sequencing (PhIP-Seq) experiment is complete, we will apply the PhIP-Seq assay to the entire set of >200 breast cancer samples and healthy volunteer sera that we now have in our laboratory.

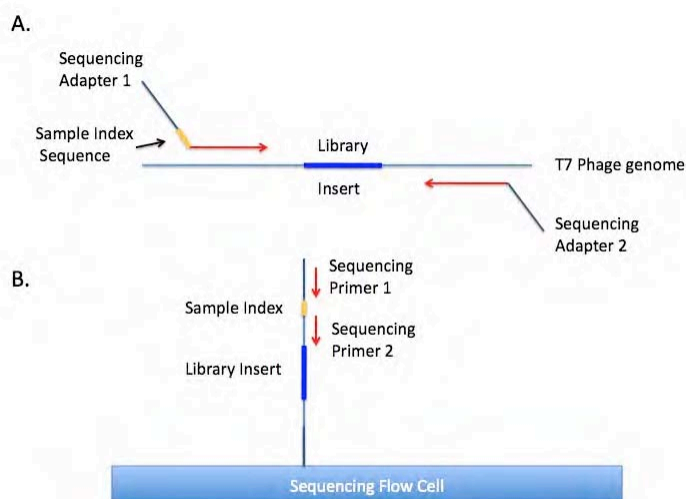


Figure 4. Indexing and sequencing strategy for the library inserts. **A.** Two primers are used to amplify the library insert from the phage genome. Both primers include adapters at their 5' ends, which are necessary for high throughput sequencing. Additionally, the forward primer contains a 4 nucleotide stretch ("indexing sequence") used to uniquely identify the sample within the multiplexed pool. **B.** The sequencing strategy to obtain the sample index and the library insert for each member of the population.

Key research accomplishments

1. Demonstration that we can perform genome-wide shRNA screens on breast lines.
2. Development of a new barcoding method that works with our version 2 libraries that gives us an ability to quickly screen libraries before their 60-mer barcodes are sequenced and the use of that method in genome-wide screens.
3. Identification of genes that are selectively toxic to multiple breast cancer cell lines.
4. Identification of several genes that appear to be synthetically lethal with ras.
5. Identification of BetaTRCP as the ubiquitin ligase that controls REST stability.
6. Generation of genome wide phage display libraries that cover the entire coding capacity of the human genome for the auto-antibody profiling and determination that IPs can be performed and enrich target phage.
7. Identification of CDYL as a bridge between REST and methyl transferases to repress gene expression and determination that CDYL suppresses cellular transformation in breast cells.

With respect to the Statement of Work, we have accomplished many of the goals of year 1, 2, 3 and 4 shown below.

Statement of Work.

Year 1.

Task 1 (Months 1-12)

In the first year we anticipate beginning to work out the conditions for using the bar coding method to follow retroviruses containing hairpins as mixtures in complex libraries. We now have a library of 22,000 hairpins covering about 8,000 genes. We will be performing exploratory screens and optimizations to test the quality of the barcoding method. We must have this method working well to carryout the synthetic lethal screens.

We accomplished this goal in two ways. The first is we performed a bar code screen for potential tumor suppressors and identified several genes described in our first report and in Westbrook et al, 2005). Secondly, we have improved our vectors to allow single copy knockdown as described in Stegmeier et al. 2005. This was absolutely essential for the bar coding experiments we have proposed to kill cancer cells.

Task 2 (Months 1-24 and possibly longer, an ongoing effort)

We will continue to expand the library during this period to encompass more genes. This will be done in collaboration with Dr. Greg Hannon.

We have accomplished this goal by the generation of a second generation library in the mir30 context as described in Silva et al., 2005. This covers 140,00 human and mouse shRNAs as was described in last years report. We have also developed new and better knockdown vectors to allow us to knock down genes with greater penetrance. Right now we feel we have nearly genome-wide coverage and are working on a new library which if successful wil be a much better and more trustworthy library.

Task 3 (Months 6-24)

We also will begin the process of analyzing the human genome for coding sequences to set up the bio-informatics analysis to generate a list of sequences we wish to express to look for auto-antibodies. We should begin synthesizing oligo nucleotides to cover human genes.

We have designed oligonucleotides to cover the human genome. We are through cloning them in phage display vectors. We are characterizing the libraries and trying to figure out how best to screen them. We ran into the problem that screening them by microarray ran into cross hybridization problems which we are addressing bioinformatically.

Year 2.

Task 4 (Months 13-24)

In this period we plan to begin to carryout screen to look for genes which when knocked down by shRNA will interfere with the growth of cells containing defined mutations that lead to breast cancer. We will start with known tumor suppressors such as loss of p53 and Rb. We will use the barcoding methods. We may also screen for genes that sensitize cells to killing by gamma IR.

We initially tried PTEN mutants but were unable to find synthetic lethals. We have now successfully started with Kras and identified a few reproducible genes in a pilot experiment that are selectively toxic with Kras mutant cells.

Task 5 (Months 18-36)

We will begin to synthesize shRNA clones corresponding to the mouse genome.

We have completed this.

Task 6 (Months 12-24)

We will expand the library of short coding regions for the autoantibody project and work out conditions to express these protein fragments in bacteria in a high through-put fashion.

We have made the libraries and are working on developing methods to analyze the results.

Year 3.

Task 7 (Months 24-36)

We will continue to screen for synthetic lethals with tumor causing mutations relevant to breast cancer. In addition, by this time we will be retesting the synthetic lethal positives from the initial screens performed in year two.

We are in the process of performing straight lethal and synthetic lethal experiments with ras. We have carried out one screen and now hope to examine out hits in breast lines with active and inactive ras.

Task 8 (Months 24-36)

We plan to work out the conditions for placing the proteins expressing short segments of human proteins for the auto-antibody screening project onto glass slides for screening purposes.

We have abandoned this aim in that we switched our approach to a phage display library which does not require glass slide. We just made our first comprehensive library in a T7 display vector.

Task 9 (Months 24-36)

We will continue to characterize the mouse shRNA library.

We are characterizing the mouse library. It was transferred into our best knockdown vector. We are in the process of performing a screen in stem cells to look for genes that enhance ionizing radiation resistance or sensitivity.

Years 4 and 5.

These years are listed together as they will be consumed with executing the long-term goals of the Tasks outlined in years 1 through 3.

Task 10 (Months 36-60)

We will begin to screen human sera for autoantibodies against our arrays of human protein fragments. We will work out these methods and attempt to begin a higher through-put analysis to determine if common epitopes are eliciting a response in breast cancer patients.

We have made the libraries and obtained the sera samples. In this year we have established the that the methods should work with reconstruction experiments and are working out ways to screen the data generated. We will not be able to use miroarray readouts because of cross hybriuzation and will be looking into sequencing..

Task 11 (Months 36-60)

We will infect mice with retroviral libraries and screen for tumor suppressors in the breast and possibly other tissues.

We have not gotten to the point where we can do this aim as we are consumed with finding the cancer the lethals.

Task 12 (Months 36-60)

We will be examining the genes we have found in various screens using standard molecular biological approaches to understand their roles in control of the responses we screened for in previous tasks.

We are doing this with some of our tumor suppressor hits and some potential oncogenes we have found. We are following up on the cancer-specific lethals as well as ras synthetic lethals. The ras synthetic lethals appear to be falling into a pathway that reveals that ras is sensitive to mitotic perturbation.

Reportable outcomes

Westbrook, T.F., Hu, G., Ang, X.L., Mulligan, P., Pavlova, N.N., Liang, A., Leng, Y., Maehr, R., Shi, Y., Harper, W.J., and Elledge, S.J. (2008) SCF-bTRCP Controls Oncogenic Transformation and Neural Differentiation Through REST Degradation. *Nature* 452:370-4.

Mulligan, P., Westbrook, T.F., Ottinger, M., Pavlova, N., Chang, B., Macia, E., Shi, Y.J., Barretina, J., Liu, J., Howley, P.M., Elledge, S.J., Shi, Y. (2008) CDYL bridges REST and histone methyltransferases for gene repression and suppression of cellular transformation. *Mol Cell* 32:718-26.

Conclusions

Progress on understanding the REST Tumor suppressor pathway.

It is clear that REST acts as a tumor suppressor in mammary cells. That means that the pathways controlling REST are also likely to be important in tumor suppression as well. We have discovered a new protein kinase driven pathway that targets REST for proteolytic degradation via the SCF using the F-box protein BTRCP. Since BTRCP overproduction is oncogenic and causes cellular transformation through REST degradation, we have now established a cellular transformation pathway that links a known oncogene to the negative control of a tumor suppressor gene,

Progress on barcode screening for essential genes

It is clear from our current studies that we have overcome the main problem with performing barcode screens which is getting sufficiently good knockdown from single copy vectors and being able to reproducibly measure their abundance in complex pools by microarray hybridization. We have now gone most way through a genome screen for cancer-specific lethals in three genetically distinct breast cancer lines. This has been our major goal from the very start and we are now verifying the results and determining which are truly cancer specific. In addition, we have begun a screen to find genes that are synthetically lethal with Kras mutations. We hope to start cMyc and PI3K synthetic lethals in the next year. This should tell us which mutations in the breast lines are causing the synthetic lethality we are seeing.

Screens for Tumor suppressors using the RNAi library and for Oncogenes using the ORFeome library

We originally thought last year that this ongoing effort should be completed in the next year. However, we ran into trouble with our cell transformation assay. Apparently the supplier of our specialized media for HMECs switched some of their components and nothing worked. We worked hard for 6 months and thought we had finally overcome that problem which is important for both the shRNA screens as well as the overproduction screens for oncogenes but we were wrong and still have a problem. We think we may be back on track but it will be a while. But we have now constructed new shRNA libraries that have 12 hairpins per gene which we will screen using HMECs if possible.

In addition we are performing the same screens with retroviral ORFeome libraries which are the equivalent to normalized full length cDNA libraries. One gene we are following up is PVRL4/Nectin-4. It potently transforms HMECs and is overproduced in 62% of ductal carcinomas. We have found several breast lines that express PVRL4 and when it is knocked down the cells show reduced proliferation and no longer grow in clumps like stem cells. We hope to have a paper on this next year.

Investigation of Auto-Antibodies as Breast Cancer Biomarkers

We are still in early stages of this project but we now have the libraries in hand and the patient samples. We have run into read-out problems on the microarrays because we are forced to use the sequences that are coded as opposed to optimized barcodes. We are trying to optimize the probes on the microarray to limit cross hybes and we still have a lot of cross hybe problems so we are trying to reduce the cost of sequencing using multiplex strategies. This remains a major limitation.

References

1. Chong, J. A. et al. REST: a mammalian silencer protein that restricts sodium channel gene expression to neurons. *Cell* **80**, 949-57 (1995).
2. Schoenherr, C. J. & Anderson, D. J. The neuron-restrictive silencer factor (NRSF): a coordinate repressor of multiple neuron-specific genes. *Science* **267**, 1360-3 (1995).
3. Ballas, N. & Mandel, G. The many faces of REST oversee epigenetic programming of neuronal genes. *Curr Opin Neurobiol* **15**, 500-6 (2005).
4. Westbrook, T. F. et al. A genetic screen for candidate tumor suppressors identifies REST. *Cell* **121**, 837-48 (2005).
5. Ballas, N., Grunseich, C., Lu, D. D., Speh, J. C. & Mandel, G. REST and Its Corepressors Mediate Plasticity of Neuronal Gene Chromatin throughout Neurogenesis. *Cell* **121**, 645-57 (2005).
6. Petroski, M. D. & Deshaies, R. J. Function and regulation of cullin-RING ubiquitin ligases. *Nat Rev Mol Cell Biol* **6**, 9-20 (2005).
7. Bai, C. et al. SKP1 connects cell cycle regulators to the ubiquitin proteolysis machinery through a novel motif, the F-box. *Cell* **86**, 263-74 (1996).
8. Skowyra, D., Craig, K. L., Tyers, M., Elledge, S. J. & Harper, J. W. F-box proteins are receptors that recruit phosphorylated substrates to the SCF ubiquitin-ligase complex. *Cell* **91**, 209-19 (1997).
9. Guardavaccaro, D. et al. Control of meiotic and mitotic progression by the F box protein beta-Trcp1 in vivo. *Dev Cell* **4**, 799-812 (2003).
10. Shirogane, T., Jin, J., Ang, X. L. & Harper, J. W. SCFbeta-TRCP controls clock-dependent transcription via casein kinase 1-dependent degradation of the mammalian period-1 (Per1) protein. *J Biol Chem* **280**, 26863-72 (2005).
11. Busino, L. et al. Degradation of Cdc25A by beta-TrCP during S phase and in response to DNA damage. *Nature* **426**, 87-91 (2003).
12. Jin, J. et al. SCFbeta-TRCP links Chk1 signaling to degradation of the Cdc25A protein phosphatase. *Genes Dev* **17**, 3062-74 (2003).
13. Winston, J. T. et al. The SCFbeta-TRCP-ubiquitin ligase complex associates specifically with phosphorylated destruction motifs in IkappaBalpha and beta-catenin and stimulates IkappaBalpha ubiquitination in vitro. *Genes Dev* **13**, 270-83 (1999).
14. Fuchs, S. Y., Spiegelman, V. S. & Kumar, K. G. The many faces of beta-TrCP E3 ubiquitin ligases: reflections in the magic mirror of cancer. *Oncogene* **23**, 2028-36 (2004).
15. Wu, G. et al. Structure of a beta-TrCP1-Skp1-beta-catenin complex: destruction motif binding and lysine specificity of the SCF(beta-TrCP1) ubiquitin ligase. *Mol Cell* **11**, 1445-56 (2003).

16. Zhao, J. J. et al. Human mammary epithelial cell transformation through the activation of phosphatidylinositol 3-kinase. *Cancer Cell* **3**, 483-95 (2003).
17. Kudo, Y. et al. Role of F-box protein betaTrcp1 in mammary gland development and tumorigenesis. *Mol Cell Biol* **24**, 8184-94 (2004).
18. Nishikawa, S., Jakt, L. M. & Era, T. Embryonic stem-cell culture as a tool for developmental cell biology. *Nat Rev Mol Cell Biol* **8**, 502-7 (2007).
19. Ying, Q. L., Stavridis, M., Griffiths, D., Li, M. & Smith, A. Conversion of embryonic stem cells into neuroectodermal precursors in adherent monoculture. *Nat Biotechnol* **21**, 183-6 (2003).
20. Aubert, J. et al. Screening for mammalian neural genes via fluorescence-activated cell sorter purification of neural precursors from Sox1-gfp knock-in mice. *Proc Natl Acad Sci U S A* **100 Suppl 1**, 11836-41 (2003).
21. Bain, G., Kitchens, D., Yao, M., Huettner, J. E. & Gottlieb, D. I. Embryonic stem cells express neuronal properties in vitro. *Dev Biol* **168**, 342-57 (1995).
22. Fuller, G. N. et al. Many human medulloblastoma tumors overexpress repressor element-1 silencing transcription (REST)/neuron-restrictive silencer factor, which can be functionally countered by REST-VP16. *Mol Cancer Ther* **4**, 343-9 (2005).
23. Su, X. et al. Abnormal expression of REST/NRSF and Myc in neural stem/progenitor cells causes cerebellar tumors by blocking neuronal differentiation. *Mol Cell Biol* **26**, 1666-78 (2006).
24. Saitoh, T. & Katoh, M. Expression profiles of betaTRCP1 and betaTRCP2, and mutation analysis of betaTRCP2 in gastric cancer. *Int J Oncol* **18**, 959-64 (2001).
25. Noubissi, F. K. et al. CRD-BP mediates stabilization of betaTrCP1 and c-myc mRNA in response to beta-catenin signalling. *Nature* **441**, 898-901 (2006).